Spin quantum Hall effect in unconventional superconductors

T. Senthil
Institute for Theoretical Physics, University of California, Santa Barbara, California 93106-4030

J. B. Marston
Institute for Theoretical Physics, University of California, Santa Barbara, California 93106-4030
*and Department of Physics, Brown University, Providence, Rhode Island 02912-1843**

Matthew P. A. Fisher
Institute for Theoretical Physics, University of California, Santa Barbara, California 93106-4030
(Received 4 February 1999)

We study the properties of the ''spin quantum Hall fluid''—a spin phase with quantized spin Hall conductance that is potentially realizable in superconducting systems with unconventional pairing symmetry. A simple realization is provided by a $d_{x^2-y^2}+id_{xy}$ superconductor which we argue has a dimensionless spin Hall conductance equal to 2. A theory of the edge states of the $d_{x^2-y^2}+id_{xy}$ superconductor is developed. The properties of the transition to a phase with vanishing spin Hall conductance induced by disorder are considered. We construct a description of this transition in terms of a supersymmetric spin chain, and use it to numerically determine universal properties of the transition. We discuss various possible experimental probes of this quantum Hall physics. [S0163-1829(99)00426-9]

I. INTRODUCTION

A remarkable property of a singlet superconductor is the occurrence of the phenomenon of spin-charge separation.[1,2] The superconducting condensate may be viewed as a collection of spinless, charge $2e$ Cooper pairs that have Bose condensed. The spin, on the other hand, is carried entirely by the fermionic quasiparticle excitations which do not carry definite charge. This observation is particularly important in the context of superconductors with non-s-wave Cooper pairing leading possibly to quasiparticle excitations at arbitrarily low energies. The best studied case is $d_{x^2-y^2}$ pairing in the high-T_c cuprates. The resulting superconducting state has gapless quasiparticle excitations which dominate the low-temperature properties. The cuprates thus provide an opportunity to explore the low-energy properties of a gapless spin-charge separated system in dimensions greater than 1. Recent work[3,4] has pointed out the possibility of realizing a novel spin phase—the ''spin metal''—in the cuprates in the presence of disorder. This phase is characterized by a nonvanishing finite spin-diffusion constant and spin susceptibility at zero temperature, and is not known to exist in insulating Heisenberg spin models. In this work, we explore another spin phase potentially realizable in superconducting systems—the ''spin quantum Hall fluid.'' This phase is characterized by a quantized value of the Hall spin conductance (analogous to the quantized Hall charge conductance in the integer quantum Hall effect).

We begin by showing that such a spin quantum Hall fluid phase is realized by two-dimensional superconductors with $d_{x^2-y^2}+id_{xy}$ symmetry. The $d+id$ state, which has received a fair amount of attention recently,[5–8] has been known to possess various similarities with quantum Hall states, though the precise characterization in terms of spin transport has not been pointed out before. In particular, it has been suggested that a transition from the $d_{x^2-y^2}$ to the $d_{x^2-y^2}+id_{xy}$ superconductor may be driven by external magnetic fields,[6] and hence is potentially realizable in the cuprates.

Here we first calculate the bulk spin Hall conductance of the $d+id$ state and show explicitly that it is quantized to be equal to 2 (in units of the dimensionless spin conductance). We then use semiclassical arguments to show the existence of two spin-current carrying edge states as required by the quantization of the bulk Hall spin conductance. A Hamiltonian describing the propagating edge modes is derived. We next consider the effects of disorder on the $d+id$ state. The quantization of the spin Hall conductance is robust to weak impurity scattering. However, if the impurity scattering is sufficiently strong, there can be a phase transition to a phase with vanishing Hall spin conductance. The properties of this transition are considered next. Ignoring the quasiparticle interactions, this transition is argued to be described by the critical point of a replica nonlinear sigma model theory[3] with a topological term which describes quasiparticle localization in a superconductor without time reversal but with spin rotation invariance (class C of Ref. 9). We then construct a network model[10] describing this transition, and show that it is identical to that simulated recently by Kagalovsky *et al.*[11] We then motivate a description of this transition in terms of a supersymmetric (SUSY) spin chain. In contrast to the SUSY spin chain which describes the usual integer quantum Hall transition,[12,13] this SUSY chain has only a finite number, 3, of degrees of freedom at each site. This enables the efficient use of a numerical technique—the density-matrix renormalization group (DMRG)—which has been successfully used for accurate calculations of the properties of quantum spin chains in other situations.[14] We present numerical results for a number of universal critical properties of the transition. Some of these have been obtained before from the network model simulations.[11] Very recently, Gruzberg, Lud-

wig, and Read[15] have provided a mapping of this transition to classical percolation and determined exact values for various critical exponents. Our numerical results are in excellent agreement with these exact values. We conclude with a general discussion of various experimental probes of the physics discussed in this paper.

II. BULK SPIN HALL CONDUCTANCE OF THE $d+id$ SUPERCONDUCTOR

We begin by defining the spin Hall conductance. In general, the spin conductance measures the spin current induced in the system in response to a spatially varying Zeeman magnetic field. The spin Hall conductance measures the spin current in a direction transverse to the direction of variation of the external Zeeman field. More precisely, a Zeeman field $B^z(y)$ along, say the z direction of spin, which depends only on, for instance, the spatial y direction, leads to a current j_x^z of the z component of the spin along the spatial x direction given by

$$j_x^z = \sigma_{xy}^s \left(-\frac{dB^z(y)}{dy} \right) \tag{1}$$

with σ_{xy}^s being the spin Hall conductance. (Note that the analog of the ''electric'' field for spin transport is the derivative of the Zeeman field.) Just like the usual Hall effect, σ_{xy}^s is 0 in the presence of parity and time-reversal invariances. The $d+id$ superconductor is neither parity nor time-reversal invariant and hence can have a nonvanishing σ_{xy}^s.

Before proceeding further, it is worthwhile to recall some general properties of singlet superconductors with no time-reversal invariance. Consider a general lattice BCS Hamiltonian for such a superconductor:

$$\mathcal{H} = \sum_{i,j} \left[t_{ij} \sum_{\alpha} c_{i\alpha}^\dagger c_{j\alpha} + \Delta_{ij} c_{i\uparrow}^\dagger c_{j\downarrow}^\dagger + \Delta_{ij}^* c_{j\downarrow} c_{i\uparrow} \right], \tag{2}$$

where i,j refer to the sites of some lattice. Hermiticity implies $t_{ij} = t_{ji}^*$, and spin rotation invariance requires $\Delta_{ij} = \Delta_{ji}$.

It is often useful to use an alternate representation in terms of a new set of d operators defined by

$$d_{i\uparrow} = c_{i\uparrow}, \quad d_{i\downarrow} = c_{i\downarrow}^\dagger. \tag{3}$$

The Hamiltonian, Eq. (2), then takes the form

$$\mathcal{H} = \sum_{ij} d_i^\dagger \begin{pmatrix} t_{ij} & \Delta_{ij} \\ \Delta_{ij}^* & -t_{ij}^* \end{pmatrix} d_j \equiv \sum_{ij} d_i^\dagger H_{ij} d_j. \tag{4}$$

Writing $t_{ij} = a_{ij}^z + i b_{ij}$, $\Delta_{ij} = a_{ij}^x - i a_{ij}^y$ with $\vec{a}_{ij} = \vec{a}_{ji}$, real symmetric, and $b_{ij} = -b_{ji}$, real antisymmetric, gives

$$H_{ij} = i b_{ij} + \vec{a}_{ij} \cdot \vec{\sigma}, \tag{5}$$

where $\vec{\sigma}_i$ are the three Pauli matrices. Note that $SU(2)$ spin rotational invariance requires

$$\sigma_y H_{ij} \sigma_y = -H_{ij}^*. \tag{6}$$

Equivalently, we may require that the second quantized Hamiltonian $\mathcal{H}$ in Eq. (4) be invariant under

$$d \to i \sigma_y d^\dagger. \tag{7}$$

The advantage of going to the d representation is that the Hamiltonian conserves the number of d particles. Note that the transformation Eq. (3) implies that the number of d particles is essentially the z component of the physical spin density:

$$S_i^z = \frac{\hbar}{2} (d_i^\dagger d_i - 1). \tag{8}$$

A spin rotation about the z axis corresponds to a $U(1)$ rotation of the d operators. This $U(1)$ is clearly present in the d Hamiltonian. Invariance under spin rotations about the x or y axes is not manifest though.

Now consider the particular case of a $d_{x^2-y^2} + i d_{xy}$ superconductor.[17] In momentum space, the Hamiltonian is

$$\mathcal{H} = \sum_{k\alpha} \epsilon_k c_{k\alpha}^\dagger c_{k\alpha} + (\Delta_k c_{k\uparrow}^\dagger c_{-k\downarrow}^\dagger + \text{H.c.}), \tag{9}$$

where ϵ_k is the band dispersion and $\Delta_k = \Delta_0 \cos(2\theta_k) - i\Delta_{xy} \sin(2\theta_k)$ with $\tan(\theta_k) = k_y/k_x$. It is sometimes useful to think in terms of a lattice version of the $d+id$ superconductor. This has been formulated by Laughlin.[6] Translating to momentum space, for a square lattice, we have $\epsilon_k \sim [\cos(k_x) + \cos(k_y)]$, $\Delta_k \sim \Delta_0 [\cos(k_x) - \cos(k_y)] - i\Delta_{xy} \sin(k_x) \sin(k_y)$ which has the same symmetry under fourfold rotations of the lattice as the form written down earlier.

The parameter Δ_{xy} measures the relative strength of the d_{xy} and $d_{x^2-y^2}$ components. $\Delta_{xy} = 0$ corresponds to the familiar $d_{x^2-y^2}$ state. In this limit, the gap function Δ_k vanishes at four points of the Fermi surface and there are gapless quasiparticle excitations at these four nodes. A low-energy theory of the $d_{x^2-y^2}$ superconductor can be obtained[2] by linearizing the dispersion relation of these quasiparticles around the nodes. We put $\Upsilon_1(k) = c_k$, $\Upsilon_2(k) = i\sigma_y c_{-k}^\dagger$ for $k_y > 0$ to write

$$\mathcal{H} = \sum_k{}' \Upsilon^\dagger(k) (\epsilon_k \tau_z + \Delta_k \tau_x) \Upsilon(k), \tag{10}$$

where the prime indicates a sum over $k_y > 0$ and $\vec{\tau}$ are the Pauli matrices in Υ_1, Υ_2 (particle-hole) space. If (K_1, K_2) are the two nodal directions with $k_y > 0$, we may just keep modes near (K_1, K_2). Linearizing ϵ_k and Δ_k near the nodes, we get the following low-energy theory for the $d_{x^2-y^2}$ superconductor:

$$\mathcal{H} = \int d^2X \psi_1^\dagger (-i v_F \partial_X \tau_z + i v_\Delta \partial_Y \tau_x) \psi_1 + (1 \leftrightarrow 2; X \leftrightarrow Y). \tag{11}$$

Here $X = 1/\sqrt{2}(x+y)$ and $Y = 1/\sqrt{2}(-x+y)$. The field ψ_i is the Fourier transform of $\psi_i(k) = \Upsilon(K_i + k)$ for $i = 1,2$. Each ψ_i thus has four components $\psi_{ia\alpha}$ where a is the particle-hole index and α the spin index. The ψ_i transform as spinors under $SU(2)$ spin rotations. This Hamiltonian is manifestly invariant under spin $SU(2)$. (It also has additional $U(1)$ symmetries that can be related to momentum conservation

that holds in clean systems[2]). The physical charge density is of course not conserved as is already apparent from Eq. (9).

It is useful at this stage to express the original real-space electron operators in terms of the low-energy continuum fields. This is easily seen to be

$$c_\uparrow(\boldsymbol{x}) \sim e^{i\boldsymbol{K}_j\cdot\boldsymbol{x}}\psi_{j1\uparrow} - e^{-i\boldsymbol{K}_j\cdot\boldsymbol{x}}\psi^\dagger_{j2\downarrow}, \tag{12}$$

$$c_\downarrow(x) \sim e^{i\boldsymbol{K}_j\cdot\boldsymbol{x}}\psi_{j1\downarrow} + e^{-i\boldsymbol{K}_j\cdot\boldsymbol{x}}\psi^\dagger_{j2\uparrow}, \tag{13}$$

with a sum over the node index $(j=1,2)$ understood.

Now consider introducing a small id_{xy} component, i.e., letting $\Delta_{xy}>0$. For small Δ_{xy}, we may work with the low-energy theory Eq. (11) near the nodes of the d superconductor. The id perturbation adds to the low-energy Hamiltonian Eq. (11) the following term:

$$\mathcal{H}_{id} = \int d^2X \Delta_{xy}(\psi_1^\dagger\tau_y\psi_1 - \psi_2^\dagger\tau_y\psi_2). \tag{14}$$

Note that this is basically a mass term for the two Dirac theories describing the two nodes.

The spin density can be expressed in terms of the continuum fields as

$$\vec{S} = \frac{\hbar}{2}\psi^\dagger\vec{\sigma}\psi. \tag{15}$$

Similarly the spin currents may also be obtained from Noether's theorem.

We now perform the continuum version of the transformation Eq. (3) by defining new fields $\chi_{ia\alpha}$ through

$$\psi_{ia\uparrow} = \chi_{ia\uparrow}, \tag{16}$$

$$\psi_{ia\downarrow} = \chi^\dagger_{ia\downarrow}. \tag{17}$$

The form of the Hamiltonian Eqs. (11) and (14) is unchanged under the transformation to the χ fields. It is clear that the z component of the physical spin density is essentially the density of the χ particles. A spin rotation about the z axis corresponds to a $U(1)$ rotation of the χ fields. This $U(1)$ is clearly present in the χ Hamiltonian. Once again, invariance under spin rotations about the x or y axes is not manifest.

The d operator in real space may also be expressed in terms of these continuum fields as

$$c_\uparrow(\boldsymbol{x}) \equiv d_\uparrow(\boldsymbol{x}) \sim e^{i\boldsymbol{K}_j\cdot\boldsymbol{x}}\chi_{j1\uparrow} - e^{-i\boldsymbol{K}_j\cdot\boldsymbol{x}}\chi_{j2\downarrow}, \tag{18}$$

$$c^\dagger_\downarrow(x) \equiv d_\downarrow(\boldsymbol{x}) \sim e^{-i\boldsymbol{K}_j\cdot\boldsymbol{x}}\chi_{j1\downarrow} + e^{i\boldsymbol{K}_j\cdot\boldsymbol{x}}\chi_{j2\uparrow}, \tag{19}$$

with a sum over the node index $(j=1,2)$ understood. Note that the symmetry transformation Eq. (7) implies symmetry of the Hamiltonian under

$$\chi_{ja\alpha} \rightarrow i(\sigma_y)_{\alpha\beta}\chi^\dagger_{ja\beta}. \tag{20}$$

The calculation of the spin Hall conductance is simplified by choosing the external Zeeman field to be oriented along the z-spin direction. In that case, the spin Hall conductance is just the charge Hall conductance of the χ fields. The result is well known:[18] The contribution of each Dirac species is

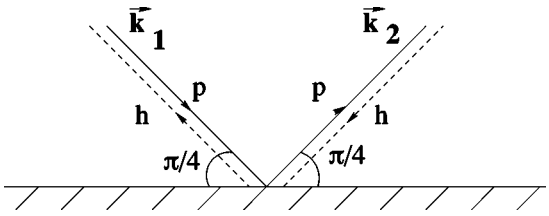

FIG. 1. Semiclassical trajectory leading to a surface bound state.

$$\frac{1}{2}\mathrm{sgn}(\Delta_{xy})\frac{(\hbar/2)^2}{2\pi\hbar}.$$

We have introduced the quantum of spin conductance $(\hbar/2)^2/2\pi\hbar = \hbar/8\pi$. As there are now four Dirac species, we obtain for the spin Hall conductance (in units of $\hbar/8\pi$) of the $d+id$ superconductor:

$$\sigma^s_{xy} = 2\ \mathrm{sgn}(\Delta_{xy}). \tag{21}$$

This is the main result of this section. (If we repeat the calculation for a $d_{x^2-y^2}+is$ superconductor, we find $\sigma^s_{xy}=0$ consistent with the analysis in the following section on edge states.)

The explicit calculation above was restricted to $|\Delta_{xy}| \ll \Delta_0$. However, the result Eq. (21) holds even away from this limit. This is because the system is in the same phase for any finite nonzero value of the ratio Δ_{xy}/Δ_0. The quantized value of the spin Hall conductance is a universal property of this phase. A topological invariant characterizing the $d+id$ phase has previously been discussed by Volovik.[16] The results of this section provided a physical interpretation of this topological invariance in terms of the quantization of the spin Hall conductance.

III. EDGE STATES

A. Semiclassical argument

As is well known from the theory of the quantum Hall effect, the quantization of the bulk spin Hall conductance implies the existence, for a system with a boundary, of spin-current carrying states at the edge. In particular, $\sigma^s_{xy}=2$ implies the existence of two such edge modes. Consider the $d+id$ superconductor with a boundary, and a particle incident on the boundary with wave vector $\vec{k}_1$ directed 45 degrees to the normal. This particle is reflected to a state with a wave vector $\vec{k}_2$ also at 45 degrees to the normal. This particle can now Andreev reflect off the bulk of the superconductor and return as a hole (see Fig. 1). The hole moves on the reverse trajectory until it is Andreev reflected from the bulk back as a particle at wave vector $\vec{k}_1$.

If the direction of $\vec{k}_1$ corresponds to an angle θ_1, the direction of $\vec{k}_2$ corresponds to angle $\theta_2 = \theta_1 \pm \pi/2$. For the $d+id$ gap $\Delta_k = \Delta_0\cos(2\theta_k) - i\Delta_{xy}\sin(2\theta_k)$. Therefore one has $\Delta_{k_1} = -\Delta_{k_2}$. Thus there is a relative phase shift of π for Andreev reflection at $\vec{k}_1$ and $\vec{k}_2$, respectively. The problem is then formally identical to that of a superconductor-normal-superconductor (SNS) junction with a phase shift of π between the two superconductors. It is well known that in such a system there exists a state at zero energy bound in the

normal layer. A similar situation obtains if the incident particle is at wave vector $-\vec{k}_2$ when again the angle of incidence is 45 degrees. For all other angles of incidence, the phase shift for the two Andreev reflections is different from π, and there is no bound state. Thus there are precisely two surface bound states for every surface orientation of the $d+id$ state. This is entirely consistent with the quantization of the bulk spin Hall conductance to be 2. This is, however, to be contrasted with the $d_{x^2-y^2}$ superconductor where the existence of such zero-energy surface states depends sensitively on the orientation of the interface.[8] Note also that for a $d_{x^2-y^2}+is$ superconductor, there is no orientation of the interface for which the phase shift for the two Andreev reflections is π—hence there are no surface bound states again consistent with the absence of a quantized spin Hall conductance.

This semiclassical argument can be made precise by solving the Bogoliubov-de Gennes (B-dG) equations for the $d+id$ superconductor in the presence of a boundary in the Andreev approximation. We remind the reader that the B-dG equations are just the eigenvalue equations for the d-particle wave functions. As the calculations are straightforward, and are very similar to those in the literature for the $d_{x^2-y^2}$ superconductor, we will not present them here. Instead, we will show how the edge modes may be obtained from the continuum theory described in the previous section.

B. Continuum Dirac theory

To show the existence of edge states within the effective low-energy Dirac theory, it is necessary that the incident and reflected modes (at 45 degrees with respect to the edge) lie along directions in momentum space which pass close to the nodes of the $d_{x^2-y^2}$ order parameter. If this is not the case, a description of the edge states requires retaining bulk modes at high energies of order Δ_0. To this end, we consider an edge parallel to the y axis located at $x=0$. It is convenient to first rewrite the Dirac Hamiltonian in the original spatial coordinates (x,y):

$$\mathcal{H}=\int d^2x\, \chi_1^\dagger[-iv\tau^x\partial_x+-i(v_x\tau^x+v_z\tau^z)\partial_y-\Delta_{xy}\tau^y]\chi_1 + (1\rightarrow 2, x\rightarrow -x, \Delta_{xy}\rightarrow -\Delta_{xy}). \tag{22}$$

Here we have performed a rotation about the τ^y axis by an angle $\theta=\arctan(v_F/v_\Delta)$ and defined $v_x=-v\cos(2\theta)$ and $v_z=v\sin(2\theta)$ with $v^2=(v_F^2+v_\Delta^2)/2$.

To establish the appropriate boundary conditions on the χ fields at $x=0$, it is necessary to use Eqs. (18) and (19) re-expressing them in terms of the underlying electron fields. As emphasized in the previous section, re-expressing the original BCS Hamiltonian in terms of the d fermions eliminates all anomalous terms, reflecting the conservation of spin, even in the presence of the edge. The appropriate boundary condition is thus simply $d_\alpha(x=0,y)=0$, which corresponds to the condition

$$\chi_{1a\alpha}(x=0,y)=-\chi_{2a\alpha}(x=0,y) \tag{23}$$

on the Dirac fields.

To search for a zero-energy edge state it is necessary to solve the wave equation which follows from the Dirac theory

$$(-iv\tau^x\partial_x-\Delta_{xy}\tau^y)\phi(x)=0, \tag{24}$$

where we have assumed the (two-component) wave function $\phi_a(x)$ is independent of y—the coordinate *along* the edge. The appropriate solution which decays into the sample for $x>0$ is readily found: $\phi_a(x)=\delta_{a1}\exp(-\Delta_{xy}x/v)$. At low energies below Δ_{xy}, the Dirac fields can be expanded in terms of this wave function as:

$$\chi_{ja\alpha}(x,y)=(-1)^j\sqrt{\frac{\Delta_{xy}}{v}}\phi_a(x)\chi_{e\alpha}(y), \tag{25}$$

with a two-component edge Fermion field $\chi_e(y)$. Here, the $(-1)^j$ factor has been included to satisfy the boundary conditions on $\chi(x=0,y)$, and the prefactor under the square root has been chosen so that the one-dimensional edge field satisfies canonical anticommutation relations. The effective edge Hamiltonian can be readily obtained by inserting this expansion into the Dirac form in Eq. (22). After performing the x integration one finds

$$\mathcal{H}_{edge}=\int dy\, \chi_{e\alpha}^\dagger(-iv_e\partial_y)\chi_{e\alpha}, \tag{26}$$

with edge velocity $v_e=v\sin(2\theta)$. For the isotropic case this implies $v_e=v_F=v_\Delta$.

The edge Hamiltonian describes a two-component one-dimensional chiral Fermion. Each edge mode contributes unity to the dimensionless Hall conductance, giving $\sigma_{xy}^s=2$. Since the edge density operator $\chi_e^\dagger\chi_e$ is proportional to the z component of spin, this is actually the *spin* Hall conductance, discussed in the previous section. Rotational invariance of the electron spin requires that the Hamiltonian be invariant under $\chi\rightarrow i\sigma_y\chi^\dagger$, or equivalently,

$$\chi_e\rightarrow i\sigma_y\chi_e^\dagger. \tag{27}$$

The edge Hamiltonian $\mathcal{H}_{edge}$ is seen to satisfy this symmetry. It is instructive to rewrite the edge Hamiltonian back in terms of the original Dirac fields ψ_α which transform as spinors under $SU(2)$ rotations. In terms of one-dimensional ''edge'' Dirac fields defined via

$$\psi_{e\uparrow}=\chi_{e\uparrow};\quad \psi_{e\downarrow}=\chi_{\downarrow e}^\dagger, \tag{28}$$

the edge Hamiltonian takes the same form:

$$\mathcal{H}_{edge}=\int dy\, \psi_e^\dagger(-iv_e\partial_y)\psi_e, \tag{29}$$

with an implicit sum on α. This form is clearly seen to be invariant under $SU(2)$ rotations $\psi_e\rightarrow U\psi_e$, with $U=\exp(i\boldsymbol{\theta}\cdot\boldsymbol{\sigma})$.

Rather surprisingly, though, the edge Hamiltonian actually is seen to have an *additional* $U(1)$ symmetry; $\psi_e\rightarrow\exp(i\theta_0)\psi_e$. This additional symmetry can be traced to the conserved $U(1)$ ''charge'' of the Dirac ψ particles—called nodons in Ref. 2. Physically, this $U(1)$ symmetry reflects the fact that the original BCS Hamiltonian conserves the *difference* between the number of electrons at one node, say at $\boldsymbol{K}_j$, and the node with opposite momentum, $-\boldsymbol{K}_j$. In the presence of impurities which break momentum conservation, this additional $U(1)$ symmetry will *not* be preserved. To see this, consider adding scattering impurities to the above edge

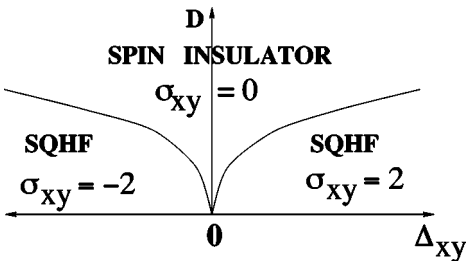

FIG. 2. Schematic phase diagram as a function of Δ_{xy} and disorder D; SQHF refers to the spin quantum Hall fluid.

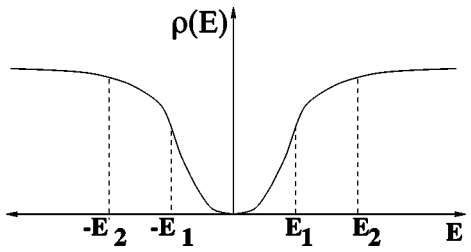

FIG. 3. Density of states of the d particles showing positions of extended states.

Hamiltonians. For impurities which do not break spin rotational invariance, the edge Hamiltonian must still be invariant under $\chi_e \rightarrow i\sigma_y \chi_e^\dagger$, and, moreover, conserve the z component of spin $\chi_e^\dagger \chi_e$. A general form satisfying these requirements is

$$\mathcal{H}_{imp} = \int dy\, \chi_e^\dagger (\boldsymbol{\eta}(y)\cdot\boldsymbol{\sigma})\chi_e , \tag{30}$$

where $\boldsymbol{\eta}(y)$ are real functions, random in the spatial coordinate along the edge. Rewritten in terms of the ψ fields these become

$$\mathcal{H}_{imp} = \int dy[\, \eta^+ \psi_e \sigma^- \psi_e + \text{H. c.} + \eta_z \psi_e^\dagger \psi_e], \tag{31}$$

with $\eta^\pm = \eta_x \pm i\eta_y$ and $\sigma^\pm = (\sigma_x \pm i\sigma_y)/2$. Although still invariant under $SU(2)$ spin rotations $\psi_e \rightarrow U\psi_e$, the additional $U(1)$ symmetry is clearly *not* present anymore, due to the anomalous ($\psi_e \sigma^- \psi_e$ and $\psi_e^\dagger \sigma^+ \psi_e^\dagger$) terms.

Although the random terms explicitly break the $U(1)$ symmetry, there is still another *hidden* $U(1)$ symmetry, which can be revealed by making a clever change of variables. Specifically, consider defining new fields

$$\tilde{\chi}_e = T_y \exp\left[\frac{i}{v_e}\int^y dy'\, \boldsymbol{\eta}(y')\cdot\boldsymbol{\sigma}\right]\chi_e , \tag{32}$$

where T_y denotes a ''time ordering'' along the spatial coordinate y. This effectively gauges away the random terms, and the full Hamiltonian when expressed in terms of the new $\tilde{\psi}_e$ fields exhibits the $U(1)$ symmetry $\tilde{\psi}_e \rightarrow \exp(i\theta_0)\tilde{\psi}_e$. This $SU(2)$ gauge transformation will play an important role in analyzing the network model studied in the next section.

IV. DISORDER EFFECTS

A. Phase diagram

We now move on to consider the effects of impurities on the $d+id$ superconductor. As shown in the previous section, the edge modes are robust to weak impurity scattering—hence so is the quantization of the bulk spin Hall conductance. Strong impurity scattering can, however, lead to a transition to a phase with zero Hall conductance. It is useful to consider a phase diagram of the system as a function of Δ_{xy} and disorder D. The general topology of such a phase diagram is shown in Fig. 2.

At zero D, $\sigma_{xy}^s = 2\,\mathrm{sgn}(\Delta_{xy})$. This spin quantum Hall phase is stable to weak disorder as seen above. The line $\Delta_{xy}=0$ is of course the $d_{x^2-y^2}$ superconductor. Turning on disorder at zero Δ_{xy} localizes the quasiparticle states at the Fermi energy[3] leading to a spin insulator. This phase should be robust to turning on a small Δ_{xy}. This is particularly clear in the lattice version of the $d+id$ superconductor in terms of the d operators. The Δ_{xy} simply corresponds to a diagonal hopping term, and hence is innocuous, if weak, in a localized phase. It is clear then that there must be two transition lines emerging from the $D=\Delta_{xy}=0$ point (symmetrically about the $\Delta_{xy}=0$ line) separating the two quantum Hall phases (with $\sigma_{xy}^s = \pm 2$) from the spin insulator with $\sigma_{xy}^s = 0$.

Note that the jump in σ_{xy}^s is by two[20]—this is prohibited in generic noninteracting models of quantum Hall systems but is allowed here due to the special extra $SU(2)$ symmetry. All phases have zero longitudinal spin conductance. It is interesting to ask about the behavior of the bulk quasiparticle density of states (DOS) $\rho(E)$ as a function of energy in various regions of the phase diagram. It is known[4] that in the spin insulator without time-reversal invariance, $\rho(E)$ actually vanishes as E^2 at low energies. In the $d+id$ superconductor, for weak disorder, standard arguments suggest the development of exponentially small tails in the density of states leading to a weak filling in of the gap. However, at disorder strong enough to be near the transition, we expect a larger density of states that nevertheless vanishes on approaching zero energy[4] as E^2.

A different perspective on the phase diagram is provided by considering the properties of the wave functions of the single-particle Hamiltonian for the d particles. In the spin quantum Hall phase, $\sigma_{xy}^s = 2$ implies the existence of precisely two extended states below the Fermi energy (each contributing unity to σ_{xy}^s). These two states will be at two different energies, say $-E_1$ and $-E_2$ (see Fig. 3). The particle-hole symmetry of the d Hamiltonian in Eq. (7) [i.e., the $SU(2)$ spin rotation invariance] implies the existence of two extended unoccupied states at positive energies E_1 and E_2. These states, if filled, contribute -1 each to σ_{xy}^s. Thus as we move up in energy and pass E_1, σ_{xy}^s jumps from 2 to 1 and finally, as we pass E_2, from 1 to 0. As the disorder increases and we approach the transition, E_1 and E_2 collapse towards zero. A nice way to move up (or down) in energy is by turning on an external Zeeman field as this acts exactly like a chemical potential for the d particles. In particular, at finite Zeeman field, the transition splits into two separate ones with σ_{xy}^s jumping by one at each. We show in Fig. 4 the phase diagram in the presence of a Zeeman field.

B. Delocalization transition

Let us now consider the properties of the transition (in zero Zeeman field) in some more detail. This is a quantum

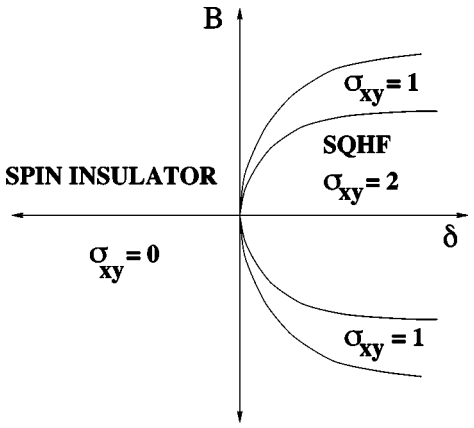

FIG. 4. Schematic phase diagram as a function of external Zeeman field B (or energy E) and a parameter δ measuring the distance (at zero field) from the zero-field phase boundary for the $0\rightarrow 2$ transition.

Hall plateau transition where σ_{xy}^{s} jumps by 2. This is a new universality class for a quantum Hall localization transition distinct from the usual one described (for instance) by the Chalker-Coddington network model. A field-theoretic description of this critical point in two-dimensional superconductors without time reversal but with spin rotation symmetry is obtained on examining the nonlinear sigma model appropriate for describing quasiparticle localization in such a system. In a replica formalism, this is a sigma model on the space $Sp(2n)/U(n)$.[3,4,19] This field theory admits a topological term[3] as $\Pi_2(Sp(2n)/U(n))=Z$ is nontrivial. We expect by analogy to the reasoning for the conventional integer quantum Hall transition that the sigma model supplemented with the topological term has a critical point which describes the spin quantum Hall transition. Introducing a Zeeman field induces a crossover to the conventional universality class.[3] This is of course consistent with the transition splitting into two as jumps of σ_{xy}^{s} by more than one are prohibited in that case. There is, however, another very significant difference between the spin quantum Hall transition and the conventional one. As mentioned above, the density of states actually vanishes (at zero energy) on either side of the transition. By continuity, we expect that the density of states vanishes at the critical point as well.

We may now formulate scaling hypotheses for various physical quantities of interest near the transition. On approaching the critical point (at zero Zeeman field) by tuning the disorder D, for instance, the localization length ξ (at zero energy) diverges as

$$\xi \sim \delta^{-\nu}, \tag{33}$$

where δ is the distance from the phase boundary. Moving away from the critical point by turning on a Zeeman field also introduces a finite localization length ξ_B diverging as

$$\xi_B \sim B^{-\nu_B}. \tag{34}$$

We may now obtain, for instance, the behavior of the density of states $\rho(E)$ at the critical point. To that end, note that moving away from zero energy is the same perturbation as turning on a Zeeman field. Consequently, the localization length as a function of energy diverges as $\xi_E \sim E^{-\nu_B}$. The density of states may now be obtained by hyperscaling:

$$\rho(E) \sim \frac{1}{E\xi_E^2} \sim E^{2\nu_B - 1}. \tag{35}$$

For $\delta \neq 0$, $\rho(E)$ satisfies the scaling form

$$\rho(E,\delta) \sim E^{2\nu_B - 1}\mathbf{Y}(E\,\delta^{-\nu/\nu_B}). \tag{36}$$

The universal scaling function $\mathbf{Y}$ satisfies

$$\mathbf{Y}(x\rightarrow\infty) = 1, \tag{37}$$

$$\mathbf{Y}(x\rightarrow 0) \sim x^{3-2\nu_B}, \tag{38}$$

where the second line follows from requiring that $\rho(E)$ vanishes as E^2 off criticality.

C. Network model

Just as for the conventional quantum Hall transition, it is possible to construct a network model to describe the universal critical properties. If we think of the links of the network model as corresponding to internal edge states of puddles of the quantum Hall fluid immersed in the spin insulator phase, then it is clear that we need to have two channels of propagation on each link. The link amplitude is the amplitude of propagation of the two channels. As the Hamiltonian H describing the dynamics of the system has the symmetry $\sigma_y H^* \sigma_y = -H$, it is clear that the unitary time evolution operator $U = e^{-iHt}$ satisfies $U^T \sigma_y U = \sigma_y$. Upon restriction to a subspace with $2N$ states, this unitary operator can be represented by a matrix belonging to the group $Sp(2N)$ (which is defined precisely as a $2N\times 2N$ unitary matrix satisfying $U^T\sigma_y U = \sigma_y$). Thus for the case of two channels, the amplitude for propagation is a 2×2 matrix belonging to the group $Sp(2) = SU(2)$. The other ingredient in the network model is the matrix at the node connecting four links. Formally, this is a scattering event with four incoming channels and four outgoing channels. The corresponding scattering matrix thus belongs to the group $Sp(4)$. Taking the link and node scattering matrices to be random and belonging to $Sp(2)$ and $Sp(4)$, respectively, then completes the specification of the network model.

In some recent work, Kagalovsky *et al.*[11] have simulated a network model with these symmetries and obtained numerical estimates of various critical exponents. Here, however, we will follow a different route. We will use the network model to motivate the construction of a supersymmetric quantum spin chain which can be used to calculate various disorder averaged properties of the system. For that purpose, it is actually more useful to consider an anisotropic version of the network model in which we view it as a collection of counterpropagating edge modes along the y direction. Two adjacent modes are connected by random tunneling. (An alternative approach to deriving a superspin chain is discussed in Ref. 15.) As shown in the previous section, each edge mode is described by a two component chiral fermion and is described by the Hamiltonian

$$(-1)^j \int dy\, \chi_j^{\dagger}(y)[-i\partial_y + \boldsymbol{\eta}_j(y)\cdot\boldsymbol{\sigma}]\chi_j(y). \tag{39}$$

Here χ_j refers to the jth edge mode. The $\boldsymbol{\eta}_j(y)$ represent the randomness on the links of the network model. To complete this Hamiltonian description of the network model, we need to introduce random tunneling between neighboring counterpropagating edge modes. The most general term consistent with the symmetries required of the Hamiltonian are

$$\sum_j \int dy\{-it_j^0(y)[\chi_{j+1}^\dagger(y)\chi_j(y)-\chi_j^\dagger(y)\chi_{j+1}(y)] + \vec{t}_j(y)\cdot[\chi_{j+1}^\dagger(y)\vec{\sigma}\chi_j(y)+\chi_j^\dagger\vec{\sigma}\chi_{j+1}]\}. \tag{40}$$

Here $t_j^0(y)$ and $\vec{t}_j(y)$ are random variables with zero mean.

Precisely this Hamiltonian for the case of just two neighboring edge modes has been studied in detail in Ref. 4. It was shown that averages of physical quantities like the density of states and diffusion propagator could be obtained from an equivalent supersymmetric quantum-mechanical problem defined by the non-Hermitian ''Hamiltonian''

$$h=h_{ff}+h_{bb}+h_{fb}+h_\omega, \tag{41}$$

$$h_{ff}=-J[(f_1^\dagger\sigma_y f_1^\dagger)(f_2^\dagger\sigma_y f_2^\dagger)+(f_1\sigma_y f_1)(f_2\sigma_y f_2) + 2(f_1^\dagger f_1-1)(f_2^\dagger f_2-1)], \tag{42}$$

$$h_{bb}=2J(b_1^\dagger b_1+1)(b_2^\dagger b_2+1), \tag{43}$$

$$h_{fb}=2J[(b_1^\dagger\sigma_y f_1^\dagger)(f_2^\dagger\sigma_y b_2^\dagger)+(b_1\sigma_y f_1)(f_2\sigma_y b_2) -(f_1^\dagger b_1)(f_2^\dagger b_2)-(b_1^\dagger f_1)(b_2^\dagger f_2)], \tag{44}$$

$$h_\omega=\omega(f_1^\dagger f_1+b_1^\dagger b_1+f_2^\dagger f_2+b_2^\dagger b_2). \tag{45}$$

Here $f_j(b_j)$ are two component fermionic (bosonic) operators, and index $j=1,2$ labels the two edge modes. Parameter ω is the imaginary frequency at which we wish to compute averages. The constant $J>0$ is determined by the strength of the disorder. Its actual value is unimportant for calculation of universal properties. We refer the reader to Ref. 4 for further details. In the following we set $J=1$ for convenience. This super-Hamiltonian generates time evolution in the y direction. Clearly the super-Hamiltonian describing the full network can be built up from this two edge Hamiltonian. Just as in the case of the superspin chain which describes the conventional quantum Hall transition,[12] the two distinct phases on either side of the transition correspond to the two possible ways of dimerizing the chain. The critical point corresponds to the uniform chain where the bond strength J is the same for all bonds. An important feature of this Hamiltonian that is not shared by superspin chains constructed for the conventional quantum Hall transition[12,13] is that the low energy sector of this theory is described by a finite on-site Hilbert space[4] of dimension $D=3$:

$$|1\rangle\equiv|0\rangle,$$

$$|2\rangle\equiv\frac{1}{\sqrt{2}}\,\epsilon_{\alpha\beta}b_\alpha^\dagger f_\beta^\dagger|0\rangle, \tag{46}$$

$$|3\rangle\equiv\frac{1}{2}\,\epsilon_{\alpha\beta}f_\alpha^\dagger f_\beta^\dagger|0\rangle.$$

This crucial simplification permits considerable numerical and analytical progress.

For a chain of L (even) sites, the super-Hamiltonian may be written, following the notation of Ref. 13, as

$$H=\sum_{j=0}^{L-2}J_j\left[\sum_{a=1}^{4}g_aS_j^aS_{j+1}^a+(-1)^j\sum_{a=5}^{8}g_aS_j^aS_{j+1}^a\right] + \sum_{j=0}^{L-1}\omega_j[S_j^1+S_j^2]. \tag{47}$$

Here $J_j=[1+(-1)^j\delta]$ where the relevant dimerization parameter $\delta=0$ at the critical point. We have introduced different imaginary frequencies ω_j at each site to permit the extraction of critical properties (see the following section). The constants g_a are defined to be

$$g_a=\begin{cases}2; & a=1,7,8\\ 1; & a=3,4\\ -2; & a=2,5,6.\end{cases} \tag{48}$$

In Eq. (47) we have introduced eight spin operators:

$$\begin{aligned} &S^1\equiv b_\alpha^\dagger b_\alpha+1, \quad S^5\equiv\epsilon_{\alpha\beta}b_\alpha^\dagger f_\beta^\dagger,\\ &S^2\equiv f_\alpha^\dagger f_\alpha-1, \quad S^6\equiv\epsilon_{\alpha\beta}b_\alpha f_\beta,\\ &S^3\equiv\epsilon_{\alpha\beta}f_\alpha^\dagger f_\beta^\dagger, \quad S^7\equiv b_\alpha^\dagger f_\alpha,\\ &S^4\equiv\epsilon_{\alpha\beta}f_\alpha f_\beta, \quad S^8\equiv f_\alpha^\dagger b_\alpha. \end{aligned} \tag{49}$$

Bosonic-valued operators $S^1,\ldots,S^4$ make up the symmetric sector of the Hamiltonian while fermion-valued operators $S^5,\ldots,S^8$ are in the antisymmetric sector. Despite the fact that H is non-Hermitian, it only has real-valued eigenvalues. H is also defective (the left eigenstates or the right eigenstates do not separately span the whole Hilbert space), complicating the numerical problem of diagonalizing it.

The Hamiltonian commutes with two (fermion-valued) supersymmetry generators, $[H,\,Q_1]=[H,\,Q_2]=0$, where

$$Q_1\equiv\sum_j\,[b_{j\alpha}^\dagger f_{j\alpha}-(-1)^j f_{j\alpha}^\dagger b_{j\alpha}],$$

$$Q_2\equiv\sum_j\,[(-1)^j b_{j\alpha}^\dagger f_{j\alpha}+f_{j\alpha}^\dagger b_{j\alpha}]. \tag{50}$$

It is not difficult to see that the supersymmetric Hamiltonian must have a unique, zero-energy ground state. The right and left (ground) eigenstates are therefore annihilated by the Hamiltonian $H|\Psi_0\rangle=\langle\Psi_0|H=0$. Also, the ground state is annihilated by the SUSY charges $Q_1|\Psi_0\rangle=Q_2|\Psi_0\rangle=0$. All excited states appear in quartets or larger multiples of 4, half with odd total fermion content, and these cancel out in the partition function by virtue of the supertrace

$$Z=\mathrm{STr}e^{-\beta H}\equiv\mathrm{Tr}(-1)^{N_f}e^{-\beta H}=1, \tag{51}$$

where N_f is the total number of fermions.

V. DMRG RESULTS

We employ the relatively simple ''infinite-size'' DMRG algorithm[14] to numerically access the properties of the critical point $\delta=0$. The fact that the ground-state energy is exactly zero provides a valuable check on the accuracy of the DMRG algorithm which incurs errors when, as the chain length increases, the Hilbert spaces of the blocks grow beyond the finite limit of M states. Increasing M up to limits set by machine memory and speed yields systematic improvement in the accuracy of the DMRG algorithm. In results reported below we have checked that M is sufficiently large to ensure adequate accuracy; for $M \geqslant 243$ there is no truncation until the chain exceeds length $L=12$. Reasonable accuracy is maintained, for the case $M=256$, out to $L=26$: the ground state, when targeted, has an energy E_0 which increases from zero to just $E_0=2.3\times10^{-4}$ at $L=26$. Furthermore, for $M=512$, the ground-state energy is only $E_0=3.2\times10^{-5}$ at chain length $L=30$, showing the systematic improvement in accuracy with increasing M.

Reduced density matrices for the two augmented blocks, each of Hilbert space size $D\times M$, are formed by computing a partial trace over half the chain. For the left half of the chain the density matrix is chosen to have the following symmetric form:[21]

$$\rho_{ij}=\frac{1}{2}\sum_{i'=1}^{DM}\{\Psi^L_{ii'}\Psi^L_{ji'}+\Psi^R_{ii'}\Psi^R_{ji'}\}; \tag{52}$$

a similar formula holds for the right half of the chain. Here $\Psi^R_{ii'}\equiv\langle i,i'|\Psi\rangle$ and $\Psi^L_{ii'}\equiv\langle\Psi|i,i'\rangle$ are, respectively, the real-valued matrix elements of the targeted right and left eigenstates projected onto a basis of states labeled by unprimed Roman index i which covers the left half of the chain and primed index i' which covers the right half. To compute ground-state properties, Ψ is selected to be the ground state; conversely, to find the gap, Ψ is chosen to be one of the lowest-lying excited states. All of the eigenvalues of ρ are real and positive; these are interpreted as probabilities and the $(D-1)M$ least probable states are thrown away.

To extract critical behavior, we monitor the induced dimerization and spin moments near the center of the chain as the chain length L is enlarged via the DMRG algorithm.[21] Dimerization is induced by the open boundary conditions as shown in Fig. 5. Spin moments are formed in the interior of the chain in two different ways. In the bulk case ω_j is set equal to a small, but nonzero, constant $\omega>0$ on each site, inducing nonzero spin moments. Alternatively, the spins at the chain ends can be fixed by setting $\omega_j=0$ except at the chain ends where ω_j is assigned a large value which completely polarizes the end spins; see Fig. 5. Power-law scaling of the induced dimerization and spin moments in the interior of the chain is expected[22] at the critical point $\delta=0$. As discussed earlier, we may move off criticality either by dimerizing the spin chain or by turning on a finite Zeeman field (which is equivalent to going away from zero energy). There are two independent exponents related to these two perturbations of the critical spin chain. As in Sec. IV, we may write down scaling forms for various physical quantities. For a finite system size, these scaling forms will involve two scaling variables: the ratio ξ/ξ_B of the two localization lengths

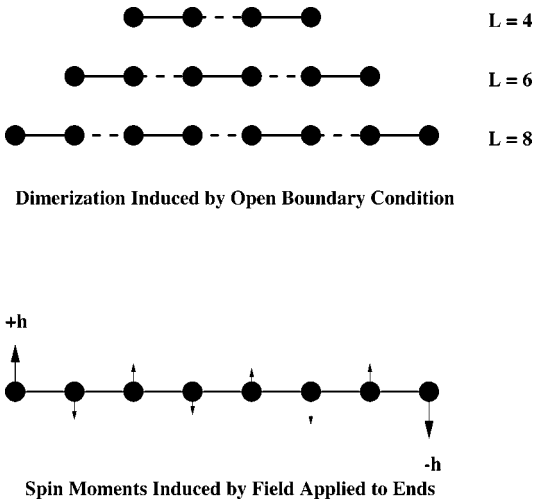

FIG. 5. Extraction of critical behavior from finite-size effects, illustrated for the case of an ordinary quantum antiferromagnetic spin chain. Dimerization of the nearest-neighbor spin-spin correlation function, indicated here by alternating strong (solid) and weak (dashed) bonds, is induced by the open boundary conditions. Spin moments are induced by the application of a magnetic field of strength $\pm h$ to the two spins at the ends of the chain (shown) or formed by the application of a staggered field throughout the chain.

and the ratio ξ/L. Consider, for instance, the density of states. This is determined by the boson occupancy according to[4]

$$2\pi\rho(E)=\frac{2}{L}\mathrm{Re}\sum_i\langle 1+b_i^\dagger b_i\rangle, \tag{53}$$

where we calculate expectation values setting $\omega_j=\omega=-i(E+i\eta)$. Thus $\rho(E)$ can be obtained from the behavior of the spin operator S^1. This scales at the center of the chain as a function of the chain length L and the uniform, ''bulk,'' imaginary frequency $\omega_j=\omega$ as follows:

$$\langle S^1_{L/2}\rangle=\omega^\alpha f(L\omega^{\nu_B},\xi\omega^{\nu_B}), \tag{54}$$

where the exponent

$$\alpha=2\nu_B-1, \tag{55}$$

as required by hyperscaling [see Eq. (35)]. When the applied dimerization $\delta=0$, this reduces to

$$\langle S^1_{L/2}\rangle=\omega^\alpha g(L\omega^{\nu_B})\sim L^y\omega \quad \text{as} \quad \omega\to0. \tag{56}$$

Here the scaling function $g(x)$ is given, for $|x|\ll1$, by

$$g(x)=x^{-\alpha/\nu_B}(c_1x^{1/\nu_B}+c_2x^{2/\nu_B}+\cdots). \tag{57}$$

This equation expresses the fact that when the system length is much smaller than the correlation length ($|x|\ll1$), the DOS is an analytic, linear function of the imaginary energy ω. With this scaling form we obtain

$$y=2(1-\nu_B)/\nu_B. \tag{58}$$

In what follows, we first describe the calculation of the exponents ν,ν_B for the two diverging localization lengths. These can then be used to extract the other critical exponents α, y using the above scaling arguments. We will, however,

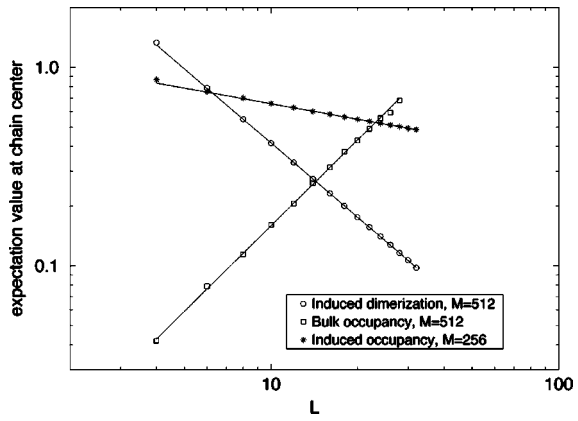

FIG. 6. Power-law scaling of the induced dimerization, the bulk occupancy, and the induced occupancy with chain length L. In the case of the induced dimerization and the bulk occupancy, $\omega_j = 10^{-5}$ throughout the chain, small enough for the bulk occupancy to be well described by the second line of Eq. (56). The bulk occupancies have been multiplied by a factor of 10^3. The induced occupancy is obtained by setting $\omega_j = 0$ everywhere except at the chain ends where it is made large, in this case $\omega_0 = \omega_{L-1} = 10$. Straight lines are fit to each of the three data sets.

provide independent support for the validity of these scaling arguments by direct calculation.

(1) Localization length exponent ν_B. The localization length scales, as a function of the imaginary frequency ω, with exponent ν_B:

$$\xi_\omega \sim \omega^{-\nu_B}. \tag{59}$$

One way to determine ν_B is to find the crossover, for uniform $\omega_j = \omega > 0$, from power-law decay of the induced dimerization to exponential decay. The induced dimerization at the center of the chain is defined as

$$\Delta(L,\omega) \equiv |\langle S^3_{L/2-1} S^3_{L/2} - S^3_{L/2} S^3_{L/2+1} \rangle|, \tag{60}$$

where we recall that $S^3 \equiv \epsilon_{\alpha\beta} f^\dagger_\alpha f^\dagger_\beta$ is one of the eight SUSY spin operators (each of the seven other spin operators scale similarly). It has the following asymptotic behavior:

$$\Delta(L,\omega) = \begin{cases} C\, L^{-x}; & \omega = 0 \\ C'\, e^{-m(\omega)L}; & m(\omega)L \gg 1. \end{cases} \tag{61}$$

Fits to the second line in Eq. (61) permit the extraction of the mass gap $m(\omega)$; then ν_B is determined by a power-law fit to $m(\omega) \sim \omega^{\nu_B}$. We find $\nu_B = 0.55 \pm 0.1$ for calculations with $M = 128$, fitting over the range $20 \leqslant L \leqslant 24$ and $0.1 < \omega < 0.8$. A direct calculation of the gap in the excitation spectrum as a function of ω also yields results consistent with this value for ν_B. Note that the exact result of Ref. 15 is $\nu_B = 4/7 = 0.5714\ldots$.

(2) Dimerization exponent ν. For small $\omega_j = 10^{-5}$, fitting the induced dimerization shown in Fig. 6 to the first line in Eq. (61) yields $x = 1.24 \pm 0.01$. The dimerization exponent ν is related to the scaling dimension x by

$$\nu = \frac{1}{2-x} \tag{62}$$

and thus $\nu = 1.32 \pm 0.02$, close to the percolation value of 4/3 reported in Ref. 15. For the spin-1/2 Heisenberg antiferromagnet and the spin-1 antiferromagnet at the critical point accuracy at the few percent level was also achieved.[21] The network model simulations[11] find $\nu \simeq 1.12$. Though this is close to the value we find numerically, and to the exact result 15, the reason for the lack of more precise agreement is unclear to us.

(3) DOS exponents α and y. Drawing upon the data shown in Fig. 6 we obtain $y = 1.43 \pm 0.05$ by direct fit of the bulk occupancy at one of the central sites to the second line of Eq. (56). The error is estimated by comparing results from DMRG calculations with $M = 256$ and $M = 512$ and also by making power-law fits over different ranges of chain lengths L. This calculation of y can now be used to calculate $\nu_B = 0.58 \pm 0.01$ in good agreement with the value obtained in item 1 above.

As mentioned above, the scaling of the DOS can be extracted in another way: set $\omega_j = 0$ everywhere along the chain except at the two sites at the ends of the chain where it is made large. Consequently at the chain ends $\langle S^1_0 \rangle = \langle S^1_{L-1} \rangle = 1$ but in the interior the expectation value $\langle S^1_{L/2} \rangle$, which we call the induced occupancy, decreases as the chain grows in length:

$$\langle S^1_{L/2} \rangle \sim \frac{1}{L^w}. \tag{63}$$

From Fig. 6 we find $w = 0.26 \pm 0.02$. Now, scaling relates $L \sim \omega^{-\nu_B}$ and hence $\alpha = w\nu_B$. Using the relation $\alpha = 2\nu_B - 1$, we get $\nu_B = 0.57 \pm 0.02$ again in agreement with the estimates above, and the exact result 15. Note that the density of states exponent $\alpha = 0.14 \pm 0.04$.

VI. DISCUSSION

How may the physics discussed in this paper be probed if a $d_{x^2-y^2} + id_{xy}$ superconductor were to be found experimentally? The bulk of this paper has focused on spin Hall transport which is extremely difficult to measure. However, the thermal Hall conductance is also quantized in the $d_{x^2-y^2} + id_{xy}$ state. This can, for instance, be seen using the edge state theory developed in Sec. III. Indeed, if the temperature of one edge is raised by δT relative to the other, the excess heat current is easily seen to be $2\pi^2 T \delta T k_B^2/3h$ implying a thermal Hall conductance of

$$\kappa_{xy} = \frac{2\pi^2 T k_B^2}{3h}. \tag{64}$$

Thus κ_{xy}/T is quantized[23] in the $d_{x^2-y^2} + id_{xy}$ superconductor. On the other hand, in the spin insulator phase, κ_{xy}/T goes to zero as the temperature goes to zero. Note that the charge Hall conductance is *not* quantized in the $d+id$ phase.[24] Physically this is because any edge quasiparticle electrical current causes flow of supercurrent in the opposite direction out to a distance of order the penetration depth.

The behavior of the quasiparticle density of states may be probed by specific-heat, spin susceptibility, or tunneling measurements. We caution, however, that it may be necessary to include quasiparticle interactions, neglected in the

theory so far, to obtain meaningful comparisons with experiments for these quantities. (The quantization of the spin and thermal Hall conductances is expected to be robust to inclusion of quasiparticle interactions.)

It is interesting to ask about experimental realizations of $d+id$ pairing symmetry in layered three-dimensional superconductors. If each layer is deep in the spin quantum Hall fluid phase, then arguments similar to those for multilayer quantum Hall systems[25,26] imply the existence of a ''chiral spin metal'' phase at the surface with diffusive spin transport in the direction perpendicular to the layers and ballistic spin transport within each layer. The properties of this chiral spin metal will be quite similar to those of the chiral metal discussed in multilayer quantum Hall systems.[25,26]

Throughout this paper, we have analyzed only the case of spin singlet pairing. For triplet pairing, such as in a *p*-wave superconductor, neither the spin nor the charge of the quasiparticles is conserved. Thermal transport still remains a useful way of probing quasiparticle transport. Arguments very similar to those used in this paper show that a two-dimensional superconductor with p_x+ip_y symmetry has a quantized thermal Hall conductance. For a layered three-dimensional system, we then have a chiral surface sheath with diffusive thermal transport in the direction perpendicular to the layers, and ballistic thermal transport within each layer. Such a layered $p+ip$ superconductor is possibly realized in the material Sr_2RuO_4.[27]

We thank Leon Balents, John Chalker, Steve Girvin, Ilya Gruzberg, Andreas Ludwig, Chetan Nayak, Nick Read, Shan-Wen Tsai, and Xiao-Gang Wen for useful discussions. This research was supported by NSF Grant Nos. DMR-9704005, DMR-9528578, DMR-9357613, DMR-9712391, and PHY94-07194. Computations were carried out with double-precision C++ code on Cray PVP machines at the Theoretical Physics Computing Facility at Brown University.

*Permanent address.

[1] S. A. Kivelson and D. S. Rokhsar, Phys. Rev. B **41**, 11 693 (1990).

[2] L. Balents, M. P. A. Fisher, and C. Nayak, Int. J. Mod. Phys. B **12**, 1033 (1998); Phys. Rev. B. **60**, 1654 (1999).

[3] T. Senthil, M. P. A. Fisher, L. Balents, and C. Nayak, Phys. Rev. Lett. **81**, 4704 (1998).

[4] T. Senthil and M. P. A. Fisher, cond-mat/9810238, Phys. Rev. B (to be published 1 September 1999).

[5] D. S. Rokhsar, Phys. Rev. Lett. **70**, 493 (1993).

[6] R. B. Laughlin, Phys. Rev. Lett. **80**, 5188 (1998).

[7] See A. V. Balatsky, Phys. Rev. Lett. **80**, 1972 (1998) for an interpretation of the experiment of R. Movshovich, M. A. Hubbard, M. B. Salamon, A. V. Balatsky, R. Yoshizaki, J. L. Sarrao, and M. Jalme, *ibid.* **80**, 1968 (1998).

[8] M. Fogelstrom, D. Rainer, and J. A. Sauls, Phys. Rev. Lett. **79**, 281 (1997); M. Covington, M. Aprili, E. Paraoanu, L. H. Greene, F. Xu, J. Zhu, and C. A. Mirkin, *ibid.* **79**, 277 (1997).

[9] A. Altland and M. R. Zirnbauer, Phys. Rev. B **55**, 1142 (1997); M. R. Zirnbauer, J. Math. Phys. **37**, 4986 (1996).

[10] J. T. Chalker and P. D. Coddington, J. Phys. C **21**, 2665 (1988).

[11] V. Kagalovsky, B. Horovitz, Y. Avishai, and J. T. Chalker, Phys. Rev. Lett. **82**, 3516 (1999).

[12] M. R. Zirnbauer, Ann. Phys. **3**, 513 (1994); N. Read (unpublished).

[13] J. B. Marston and Shan-Wen Tsai, Phys. Rev. Lett. **82**, 4906 (1999).

[14] S. R. White, Phys. Rev. Lett. **69**, 2863 (1992); Phys. Rev. B **48**, 10 345 (1993).

[15] Ilya A. Gruzberg, Andreas W. W. Ludwig, and N. Read, Phys. Rev. Lett. **82**, 4524 (1999).

[16] G. E. Volovik, Pis'ma Zh. Éksp. Teor. **66**, 492 (1997) [JETP Lett. **66**, 522 (1997)].

[17] We consider only the situation in which the gap is much smaller than the Fermi energy. There is actually another phase (''molecular limit'') in which the gap is so large that, at fixed density, the chemical potential has actually gone negative. Such a phase does not have a quantized spin Hall conductance.

[18] A. W. W. Ludwig, M. P. A. Fisher, R. Shankar, and G. Grinstein, Phys. Rev. B **50**, 7526 (1994).

[19] R. Bundschuch, C. Cassanello, D. Serban, and M. R. Zirnbauer, cond-mat/9806172 (unpublished); Phys. Rev. B **59**, 4382 (1999).

[20] This was also emphasized in Ref. 11 using the network model.

[21] J. Kondev and J. B. Marston, Nucl. Phys. B **497**, 639 (1997); Shan-Wen Tsai and J. B. Marston (unpublished).

[22] M. E. Fisher and P.-G. de Gennes, C. R. Seances Acad. Sci., Ser. B **287**, 207 (1978); F. Igloi and H. Rieger, Phys. Rev. Lett. **78**, 2473 (1997).

[23] See C. L. Kane and Matthew P. A. Fisher, Phys. Rev. B **55**, 15 832 (1997) for a discussion of quantized thermal Hall conductance in the conventional quantum Hall effect.

[24] J. Goryo and K. Ishikawa, cond-mat/9812412 (unpublished).

[25] J. T. Chalker and A. Dohmen, Phys. Rev. Lett. **75**, 4496 (1995); L. Balents and M. P. A. Fisher, *ibid.* **76**, 2782 (1996); Y.-B. Kim, Phys. Rev. B **53**, 16 420 (1996); L. Balents, M. P. A. Fisher, and M. R. Zirnbauer, Nucl. Phys. B **483**, 601 (1996); I. A. Gruzberg, N. Read, and Subir Sachdev, Phys. Rev. B **55**, 10 593 (1997); **56**, 13 218 (1997).

[26] H. L. Störmer, J. P. Eisenstein, A. C. Gossard, W. Wiegmann, and K. Baldwin, Phys. Rev. Lett. **56**, 85 (1986); D. P. Druist, P. J. Turley, K. Maranowski, E. G. Gwinn, and A. C. Gossard, *ibid.* **80**, 365 (1998).

[27] T. M. Rice and M. Sigirst, J. Phys.: Condens. Matter **7**, L643 (1995); G. M. Luke, Y. Fudamoto, K. M. Kojima, M. I. Larkin, J. Merrin, B. Nachumi, Y. J. Uemura, Y. Maeno, Z. Q. Mao, Y. Mori, H. Nakamura, and M. Sigrist, Nature (London) **394**, 558 (1998).